Examination of Local and Systemic In Vivo Responses to Electrical Injury Using an Electrical Burn Delivery System

Jeffrey W. Shupp, MD,*† Lauren T. Moffatt, PhD,* Thu Nguyen, MS,† Jessica C. Ramella-Roman, PhD,† Rasha Hammamieh, PhD,‡ Stacy-Ann Miller, BS,‡ Ellen J. Leto,* Daniel Y. Jo,* Pranay R. Randad,* Marti Jett, PhD,‡ James C. Jeng, MD,* Marion H. Jordan, MD*

Electrical injuries are devastating and are difficult to manage due to the complexity of the tissue damage and physiological impacts. A paucity of literature exists which describes models for electrical injury. To date, those models have been used primarily to demonstrate thermal and morphological effects at the points of contact. Creating a more representative model for human injury and further elucidating the physics and pathophysiology of this unique form of tissue injury could be helpful in designing stage-appropriate therapy and improving limb salvage. An electrical burn delivery system was developed to accurately and reliably deliver electrical current at varying exposure times. A series of Sprague-Dawley rats were anesthetized and subjected to injury with 1000 V of direct current at incremental exposure times (2–20 seconds). Whole blood and plasma were obtained immediately before shock, immediately postinjury, and then hourly for 3 hours. Laser Doppler images of tissue adjacent to the entrance and exit wounds were obtained at the outlined time points to provide information on tissue perfusion. The electrical exposure was nonlethal in all animals. The size and the depth of contact injury increased in proportion to the exposure times and were reproducible. Skin adjacent to injury (both entrance and exit sites) exhibited marked edema within 30 minutes. In adjacent skin of upper extremity wounds, mean perfusion units increased immediately postinjury and then gradually decreased in proportion to the severity of the injuries. In the lower extremity, this phenomenon was only observed for short contact times, while longer contact times had marked malperfusion throughout. In the plasma, interleukin-10 and vascular endothelial growth factor levels were found to be augmented by injury. Systemic transcriptome analysis revealed promising information about signal networks involved in dermatological, connective tissue, and neurological pathophysiological processes. A reliable and reproducible in vivo model has been developed for characterizing the pathophysiology of high-tension electrical injury. Changes in perfusion were observed near and between entrance and exit wounds that appear consistent with injury severity. Further studies are underway to correlate differential mRNA expression with injury severity.
(J Burn Care Res 2012;33:118–129)

Electrical injury is one of the most devastating types of trauma treated in burn centers, with more than 1000 mortalities reported annually in the United States.[1–3] Serious pathophysiological events such as cardiac arrhythmias, massive tissue destruction, compartment syndrome, and long-term neurologic dysfunction have been described with electrical injury.[1,4] In a recent study using the National Burn Repository,

*From the *The Burn Center, Department of Surgery, Washington Hospital Center, MedStar Health Research Institute, Washington, DC; †Department of Biomedical Engineering, Catholic University of America, Washington, DC; and ‡Systems and Integrative Biology, US Army Medical Command, United States Army Institute for Environmental Health Research, Frederick, Maryland.*
Presented at the 43rd annual meeting of the American Burn Association, Chicago, Illinois, March 29 to April 1, 2011.
Opinions, interpretations, conclusions, and recommendations are those of the author and are not necessarily endorsed by the U.S. Army. The views of the authors do not purport to reflect the position of the Department of the Army or the Department of Defense (Para 4-3) AR 360-5.

All animal use was carried out in accordance with AR 70-18, paragraph 12.d., in compliance with the Animal Welfare Act, adhering to the principles enunciated in the Guide for the Care and Use of Laboratory Animals.
Address correspondence to Jeffrey W. Shupp, MD, The Burn Center, Department of Surgery, Washington Hospital Center, 110 Irving Street, NW, Suite 3B-55, Washington, DC 20010.

1559-047X/2012

DOI: 10.1097/BCR.0b013e3182373a50

2837 adult patients who suffered electrical injury were identified. The majority of injuries were work-related, and the most common injury was from industrial power sources. Despite modern refinements in safety measures and regulation, electrical accidents continue to occur.

High-voltage electrical injury can cause various degrees of cutaneous damage. With this trauma comes cutaneous and connective tissue destruction to varying degrees. The severity of injury depends mainly on the current pathway and field strength through body tissues as well as duration of exposure. The main causes of damage have been identified as Joule heating, electroporation, and denaturation of membrane proteins. The hypothesized molecular mechanisms of direct injury are electrocoupled damage to structural proteins and decreased DNA synthesis.

Figure 1. Electrical burn delivery system. Plexiglass exposure chamber that is totally enclosed with ventilation fan and safety alarm that sounds upon opening (A); contact electrodes (B); power supply (C); screenshot of the control application illustrating the user interface (D).

Although wound assessment at the contact sites can be straightforward, predicting the extent of tissue damage in areas adjacent to, deep to, and between the points of contact remains difficult and unpredictable. This leads to difficulty in precise assessment of areas that require surgical excision or amputation, potentially resulting in surgeries that are too conservative or too aggressive. In addition to the traumatic injury that occurs at the electrical contact site, electric shock often results in damage at sites distant from the original injury that can be neurophysiologic, cutaneous, or involving a combination of tissues and organ systems.[5]

Furthermore, systemic pathophysiologic signaling cascades, including inflammatory mediators and host immune responses, may be initiated by current traveling through the body. This is a phenomenon that, if recognized and characterized, could improve survival due to the potential for development of refined mul-

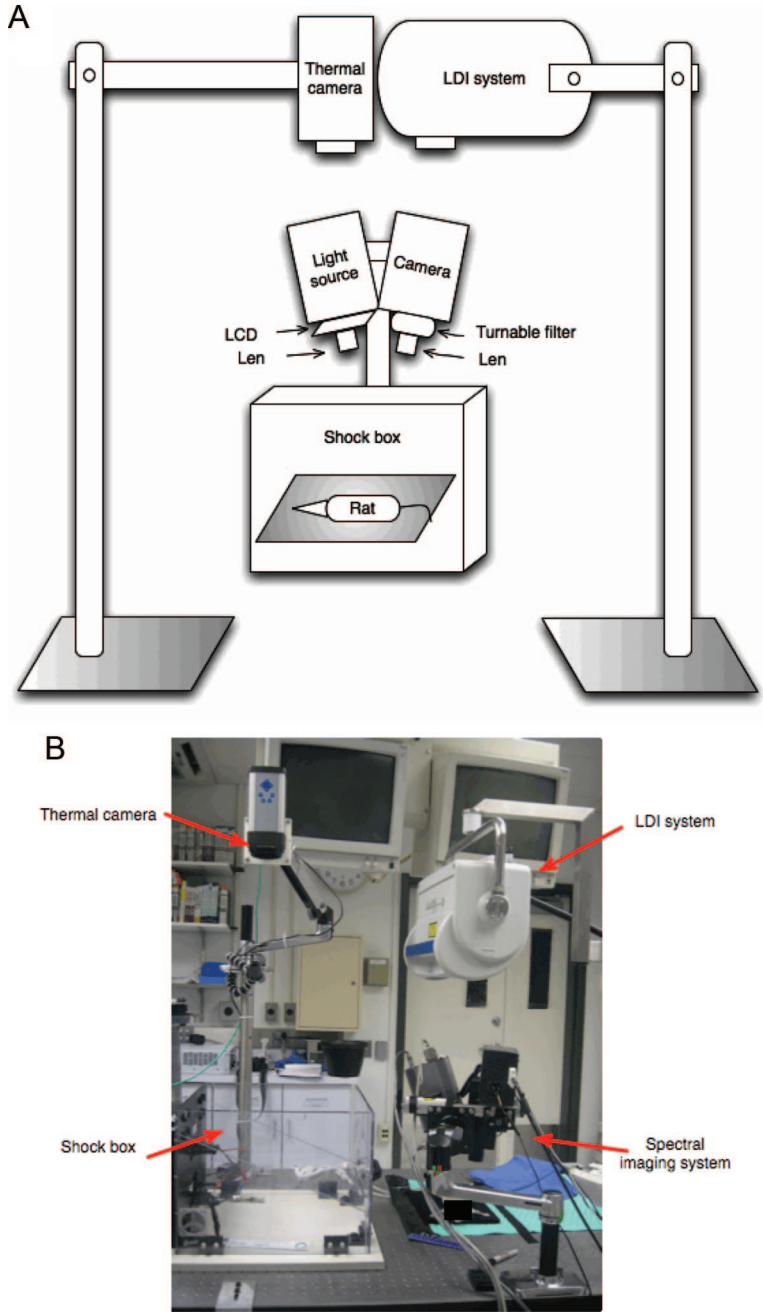

Figure 2. Composite apparatus setup. A, The design for experimental setup. B, A photograph of the actual layout.

tisystem treatment methods. Unlike the growing body of clinical evidence regarding patients who suffer thermal wounds, there is a paucity of information in the literature regarding the systemic and local responses to electrical injury.

Although few in number, studies involving animal models have been used to investigate damage to muscle and nerve tissue from electrical exposure. However, clear translational applicability is still lacking.[6–8] Furthermore, methods to deliver and measure traits of electrical shock have been tested in at least one instance on human tissue,[9] although sufficient data do not exist to determine reproducibility and applicability to an injury in an intact mammalian system.

In this study, a rat model was used to demonstrate a novel electrical burn delivery system (EBDS) of precise, controllable high-voltage direct current (DC) which creates reproducible injury. The EBDS was designed to produce burns at the contact site, as well as pathophysiologic changes in adjacent areas which could be monitored over a time course. It was hypothesized that systemic changes detectable at a molecular level would occur after injury and that these responses would be dose-dependent.

METHODS

Electrical Burn Delivery System

The EBDS was built (based on our laboratory's previous prototype) to deliver high-voltage electrical burns up to 1000 V DC to a biological load during different preset shock durations. This system consisted of an enclosed Plexiglas shock box containing two replaceable stainless steel electrodes, a controlling system including a high-voltage DC power supply (Magna-Power Electronics, Canada), a data acquisition card (Measurement Computing, Norton, MA), and a protection circuit (Figure 1). The protection circuit was built from a series of high-voltage relays which could be switched to allow high-voltage applications to the electrodes. The system was built to be safely and remotely controlled through a user interface on a computer. The user interface, written in MATLAB (Matworks, Natick, MA), supports various options of voltage and shock duration (Figure 1). Impedance measurement function was also integrated into the software, enabling a user to measure impedance as well as to observe impedance changes of a biological load at different times before and after shock. The composite experimental apparatus included the EBDS, a thermal camera, a spectral imaging system, and a laser Doppler imaging (LDI) system (Figure 2).

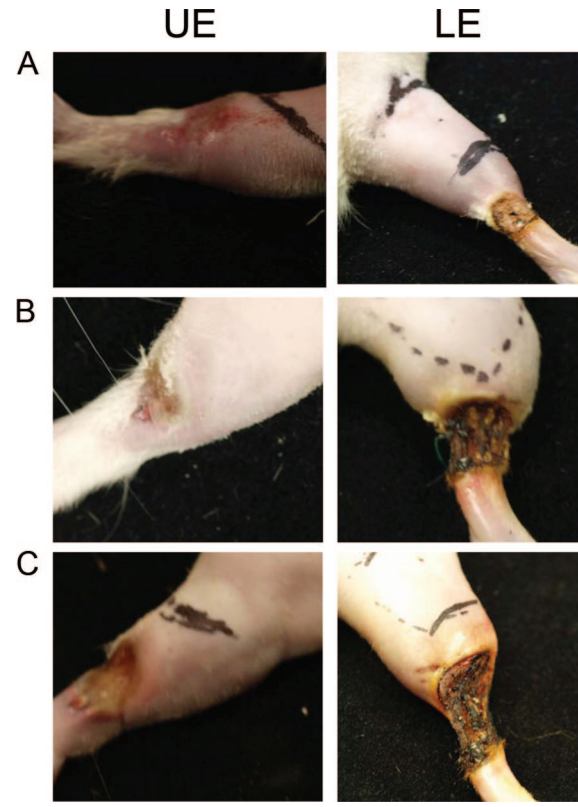

Figure 3. Representative wound photographs: 2–4 seconds (A); 6–8 seconds (B); 10–20 seconds (C).

Animal Model

The MedStar Health Research Institute's animal care and use committee approved the conduct of this research. Male Sprague-Dawley rats (Harlan Laboratories, Frederick, MD) were received through the institute's animal facility, with husbandry provided in accordance with standard operating procedures. At

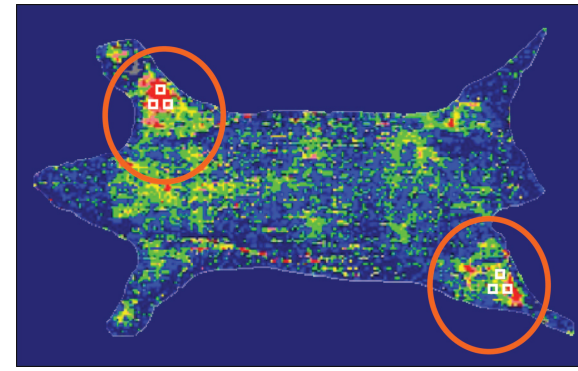

Figure 4. Heat map of an LDI scan with ROI. Representative image of a LDI scan. Orange circles indicate wound sites to be analyzed and white squares are illustrative of how ROIs were selected.

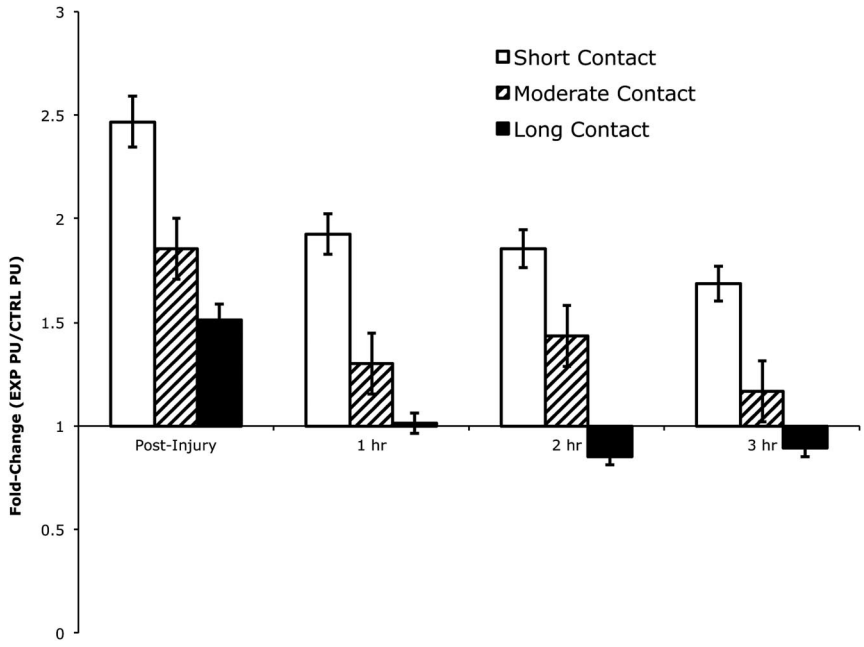

Figure 5. Upper extremity perfusion analysis. Changes in perfusion are represented as fold change. Each value represents the mean of three individual animals. Individual animal fold change was calculated by dividing the average of three ROI PU values at each time point by that of each animal's individual baseline. Error bars represent SD.

the time of experiment, animals were weighed and then tranquilized with an intramuscular injection of ketamine (10 mg/kg) and xylazine (1 mg/kg). Then, an intraperitoneal injection of urethane (150 mg/100 g) was administered for long-term anesthesia (this drug was chosen because of its duration of action and lack of cardiopulmonary suppressive side effects). Next, animals were shaved (contralat-

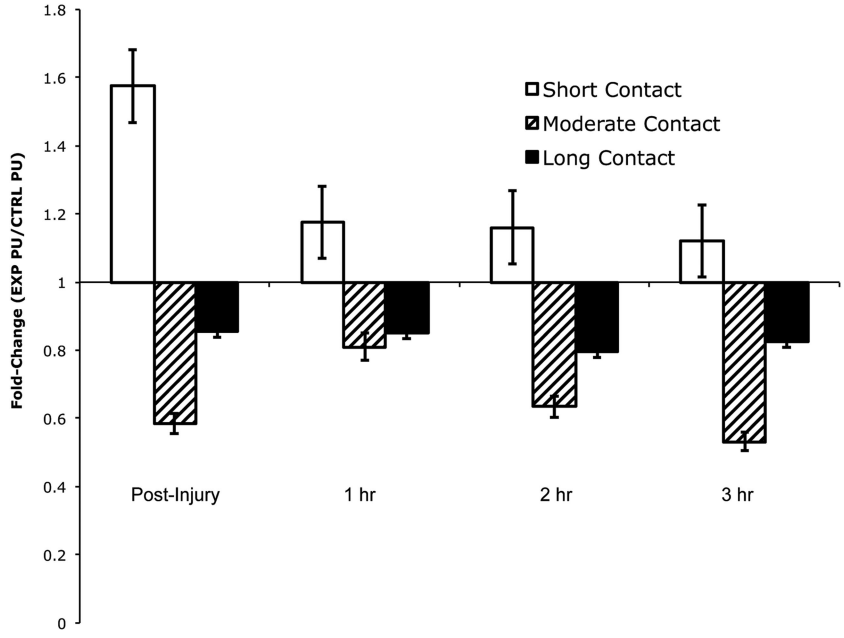

Figure 6. Lower extremity perfusion analysis. Changes in perfusion are represented as fold change. Each value represents the mean of three individual animals. Individual animal fold change was calculated by dividing the average of three ROI PU values at each time point by that of each animal's individual baseline. Error bars represent SD.

eral upper and lower extremities) using standard veterinary clippers. The extremities were then depilated with a commercial agent (Veet®, Reckitt Benckiser, Parsippany, NJ) as per laboratory standard protocol. Immediately before injury, the femoral vessels were cannulated for vascular access and pressure measurements.

Animals were then positioned prone onto a black velvet board to decrease light scattering that would obscure optical measurements. Each extremity was affixed to the velvet to prevent repositioning during transport and injury. Throughout the experiment, the plane of anesthesia was monitored, and additional drugs were administered as needed. Body temperatures were monitored every 10 minutes throughout preparation and during the entire experimental time course.

Experimental Design

Baseline images and blood samples were obtained and each animal was sequentially positioned in the EBDS with the anode electrode secured to an upper extremity and the cathode to the contralateral lower extremity. A 1000 V DC shock was delivered at times ranging from 2 to 20 seconds. A thermal camera and a video recorder captured video for the duration of the injury. After the shock, each animal was removed from the EBDS and placed on a warming blanket positioned centrally under the composite imaging apparatus. Animals were monitored for 3 hours postinjury with images captured and blood samples taken hourly. Equal volumes of warm sterile 0.9% normal saline were replaced after each blood collection. Body temperature and pedal and corneal reflexes were monitored every 10 minutes throughout. After the 3-hour time point, animals were euthanized (via exsanguination) and necropsy was immediately performed. Blood and tissue samples were recovered post-mortem and archived for future analysis.

Laser Doppler Imaging

LDI measurements of blood perfusion were obtained with the LDI2 (Moor Instruments, Devon, UK) high-frequency infrared laser beam at prescribed time points (baseline, 0, 1, 2, and 3 hours). The continuous scan mode and the smaller square scan area were selected to capture the areas adjacent to electrical injury on both upper and lower extremities. Smoothing of the LDI images was then performed to capture the underlying mean perfusion response. Regions of interest were then selected and data analyzed. Results were normalized for each animal and expressed as fold change. Stata 9.2 (StataCorp LP, College Station, Texas) was then used to conduct the following analysis. A nonparametric test for trends across ordered groups (an extension of the Wilcoxon rank-sum test) followed by a regression analysis. The model that was created had an R^2 value of 0.7 and therefore was thought to have excellent explanatory power.

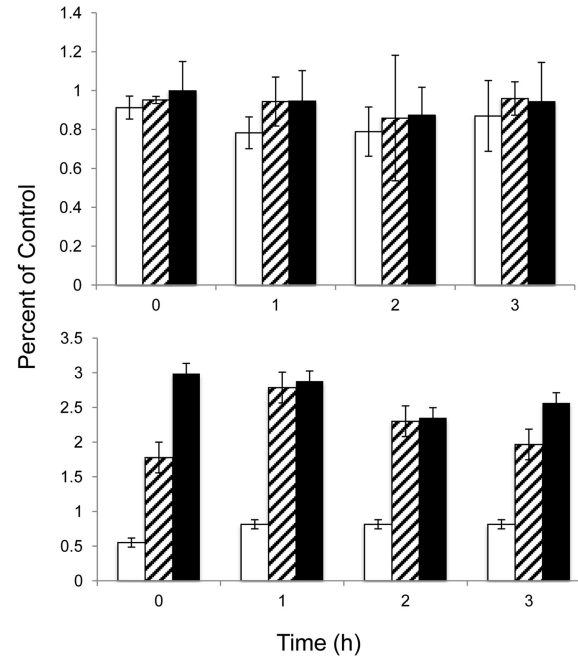

Figure 7. Plasma levels of C-reactive protein (top panel) and IL-10 (bottom panel). Changes in protein concentration are represented as percent of control and error bars represent SD. White bar = Sham; dashed bar = moderate exposure; solid bar = long exposure.

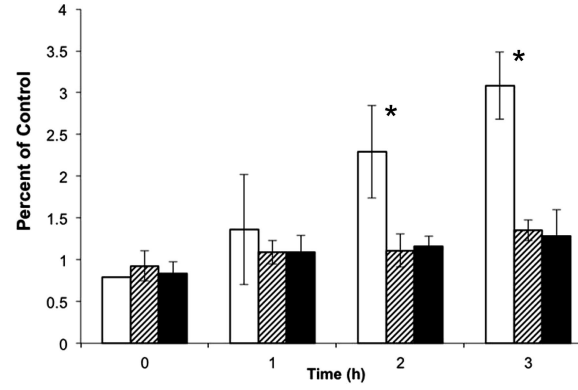

Figure 8. Plasma levels of VEGF. Changes in protein concentration are represented as percent control ± SD. Significant differences in the Sham exposure group were assessed by ANOVA followed by Scheffe's F test ($P < .05$) and are indicated by an "*". White bar = Sham; dashed bar = moderate exposure; solid bar = long exposure.

Plasma Cytokine Analysis

Whole blood was collected in Vacutainer® EDTA tubes (BD Bioscience, San Diego, CA) at prescribed time points. These 400 μl samples were centrifuged, and the resultant plasma was transferred into separate sterile tubes and stored at −80°C. Plasma cytokine concentrations were measured at Rules Based Medicine (RBM, Houston, TX) using a patented multiplex assaying system.

Gene Expression Analysis

A second 200 μl whole blood sample was drawn at the described time points and added to a sterile cry-

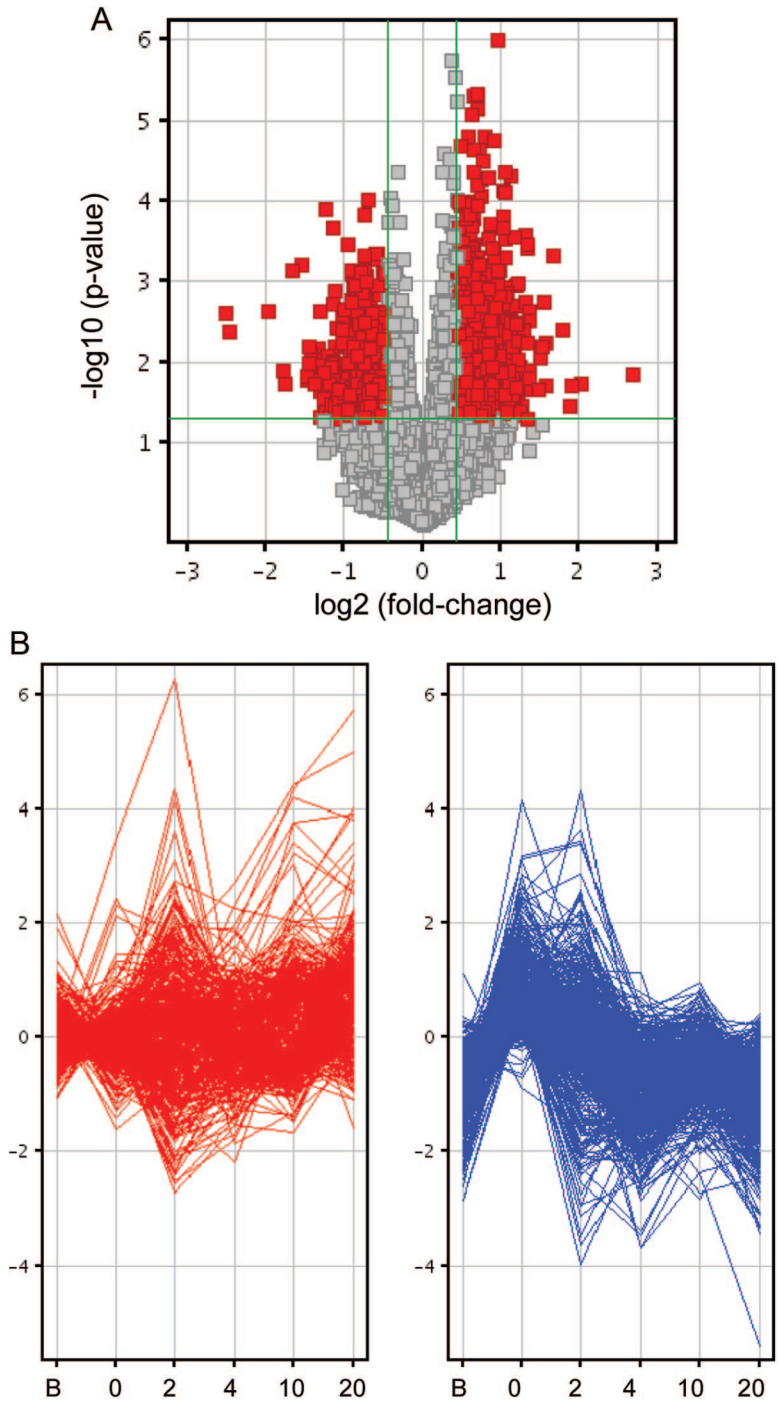

Figure 9. Differential gene expression analysis. A, Volcano plot comparing treated animals to control animals. B, Differentially up- and downregulated genes by exposure group.

ovial containing 552 μl of PAXgene Blood RNA reagent (PreAnalytiX, Qiagen GmbH, Hombrechtikon, Switzerland). Samples were mixed by inverting and allowed to incubate at room temperature for 24 hours, and then at −20°C for an additional 24 hours, with subsequent storage at −80°C until processing. High-quality RNA was isolated from thawed blood samples with the PAXgene Blood RNA kit (PreAnalytiX, Qiagen GmbH, Hombrechtikon, Switzerland) according to manufacturer's specifications. RNA samples were quantified spectrophotometrically with a Nanodrop 2000c (Thermo Fisher Scientific, Wilmington, DE). Concentrations and quality as indicated by 260/280 ratio were recorded. RNA was stored at −80°C until microarray analysis.

A representative group of RNA samples was chosen for microarray analysis to allow for a broad comparison of global gene expression between control (n = 2), short (n = 3), and long (n = 3) exposure groups while conserving remaining samples for a subsequent targeted analysis via reverse transcriptase polymerase chain reaction (RT-PCR).

Agilent 60-mer Whole Rat Genome 44k oligomicroarrays (Agilent Technologies product G4131F) printed with Agilent SurePrint technology were used for microarray analysis. RNA samples were amplified and labeled using the Agilent Low Input Quick Amp labeling Kit (part number 5190-2306) in conjunction with the Agilent Two-Color Spike-Mix (part number 5188-5279) which was added to the RNA samples before the labeling reactions according to the RNA Spike-In Kit protocol. All reactions were performed in a thermal cycler (Mycycler; Bio-Rad, Hercules, CA). Labeled samples were then subjected to fragmentation followed by 17h hybridization with the Agilent Gene Expression Hybridization Kit (part number 5188-5281). Samples were hybridized against Universal Rat Reference RNA (ID #740200, Stratagene, La Jolla, CA). Sample labeling and microarray processing were performed as outlined in the Two-Color Microarray-Based Gene Expression Analysis (version 6.5) protocol.

Microarray slides were subsequently scanned at 5-μm resolution using an Agilent G2565CA fluorescence dual laser scanner for Cy3 and Cy5 excitation.

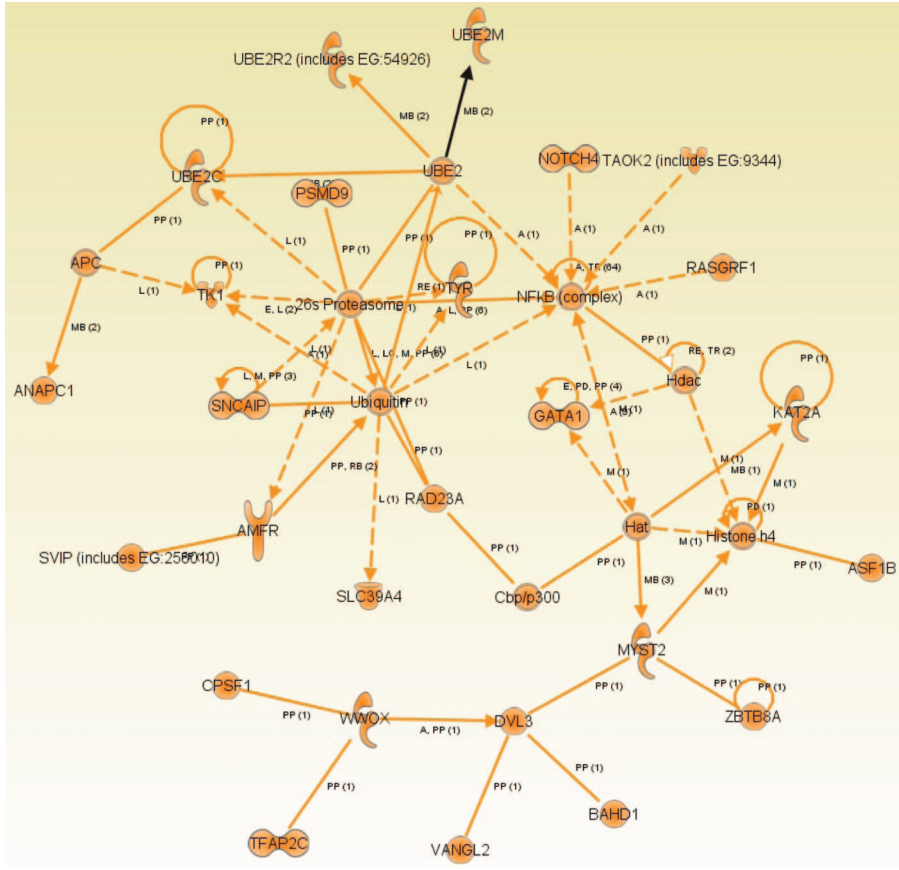

Figure 10. Dermatological disease network upregulated in injured animals.

Data were then feature extracted using default parameters in Agilent Feature Extraction Software (version 10.7.1). The aforementioned software flagged outlier features on arrays.

Microarray images were viewed and then normalized using ImaGene 6.0 (BioDiscovery, Inc., El Segundo, CA). First, data analysis was performed comparing all injured animals differential expression to that of uninjured animals. ImaGene (BioDiscovery Inc., El Segundo, CA) was used in segmenting background and foreground pixels of each spot, subsequently discarding the highest and lowest 20% groups of the probe intensity. Local background correction was applied to each spot. Genes passing this filter were further analyzed. GeneSpring 10.1 was used to carry out the data filter and statistical analysis. Intrachip normalization (LOWESS) was then done for each chip. Differentially regulated genes (between control and treated sample sets) were selected using *t*-test analysis ($P < .05$), followed by the Benjamini and Hochberg multiple correction test to find genes that varied significantly between control and treated samples with a false discovery rate of 5%.[10]

Principal component analysis was performed over the dataset to classify each sample as a statistical variable, confirming the extent of variability within the sample classes and among the predesigned groups. A two-dimensional hierarchical clustering calculation using Pearson correlation around zero was also performed.

RESULTS

Gross Examination

All animals survived the entire experiment without resuscitation. For animals that were exposed to short duration injury (2–4 seconds), lower extremity wounds (cathode) showed full-thickness injury and moderate edema in adjacent tissue. The upper extremity wounds (anode) in these animals showed partial-thickness injury and mild edema (Figure 3A). Exposure time of 10 seconds resulted in a worsening of injury in both upper and lower extremities (Figure 3B). Some of the animals exposed to current for 20 seconds had traumatic amputation of the lower limb and severe edema. Of note, the animals with longer exposure times (10–20 seconds) also exhibited myoglobinuria discovered at necropsy.

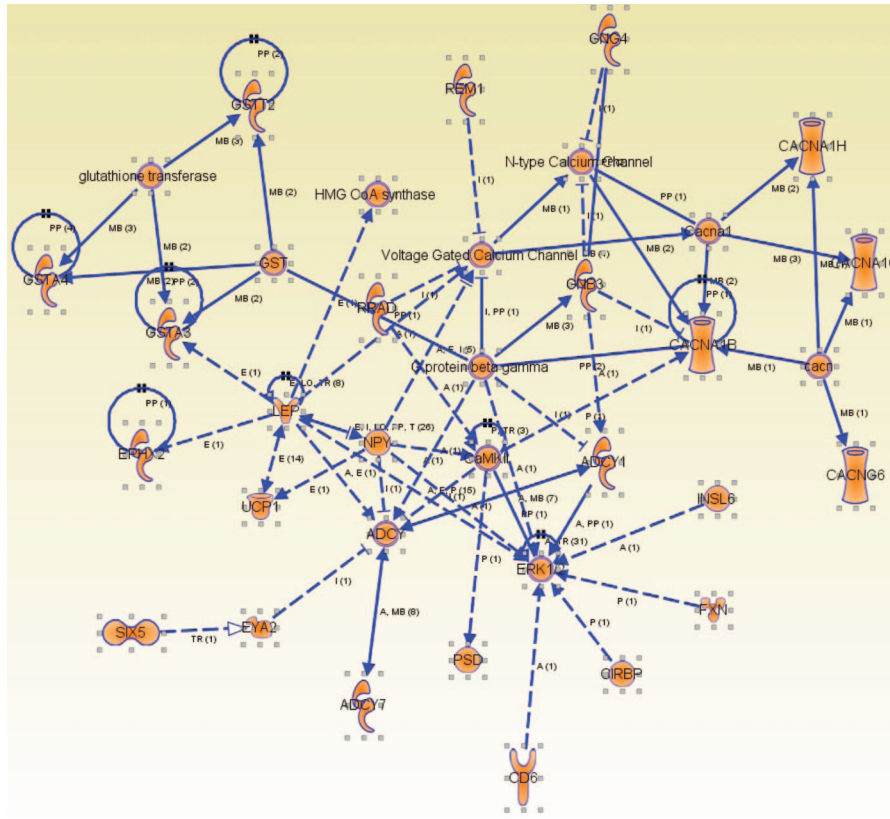

Figure 11. Connective tissue network upregulated in injured animals.

LDI Perfusion Assessments

Regions of interest were selected in the regions adjacent to injury (Figure 4). Upper extremity injuries produced a significant increase in perfusion initially after injury. This increase in perfusion dissipated over time and in the longest exposure group actually progressed to a hypoperfused state (Figure 5). In the lower extremity wounds, only the short (2–4 seconds) contact animals exhibited the biphasic response described above (Figure 6). The long (10–20 seconds) group had a significant decrease in perfusion after injury that did not rebound. The moderate exposure group's mean was significantly lower than the mean of the short exposure group ($P < .001$). The long exposure duration group's mean was significantly lower than the mean of the short exposure group ($P < .001$). The upper extremity means for all groups was higher compared with the mean of lower extremity wounds ($P < .001$). On average (for all groups and extremities and controlling for all covariates), the mean at 1 hour was lower than postinjury ($P = .002$), the mean for 2 hours was lower than postinjury ($P < .001$), and the mean for 3 hours was lower than postinjury ($P < .001$).

Plasma Cytokine Analysis

At each time point, plasma protein concentrations were assayed. Of more than 80 proteins studied, most showed no significant changes between control and injured groups C-reactive protein levels, eg, were not different between groups or time points (Figure 7A). Interleukin-10 levels were higher in treatment groups as compared with Sham animals (Figure 7B). Vascular endothelial growth factor (VEGF) levels increased over time in the Sham animals, whereas injured animals had no increase in protein levels for VEGF (Figure 8).

Gene Expression Analysis

Interchip and intrachip normalizations were applied to data using GeneSpring 10.1, as described in the Methods section. Using a one-way analysis of variance with a P value $<.05$, 1055 genes were identified that were upregulated in treated animals compared with controls, while 1445 genes were found to be downregulated as compared with controls (Figure 9A). Moreover, differential gene expression was dose-dependent when exposure groups were analyzed separately (Figure 9B).

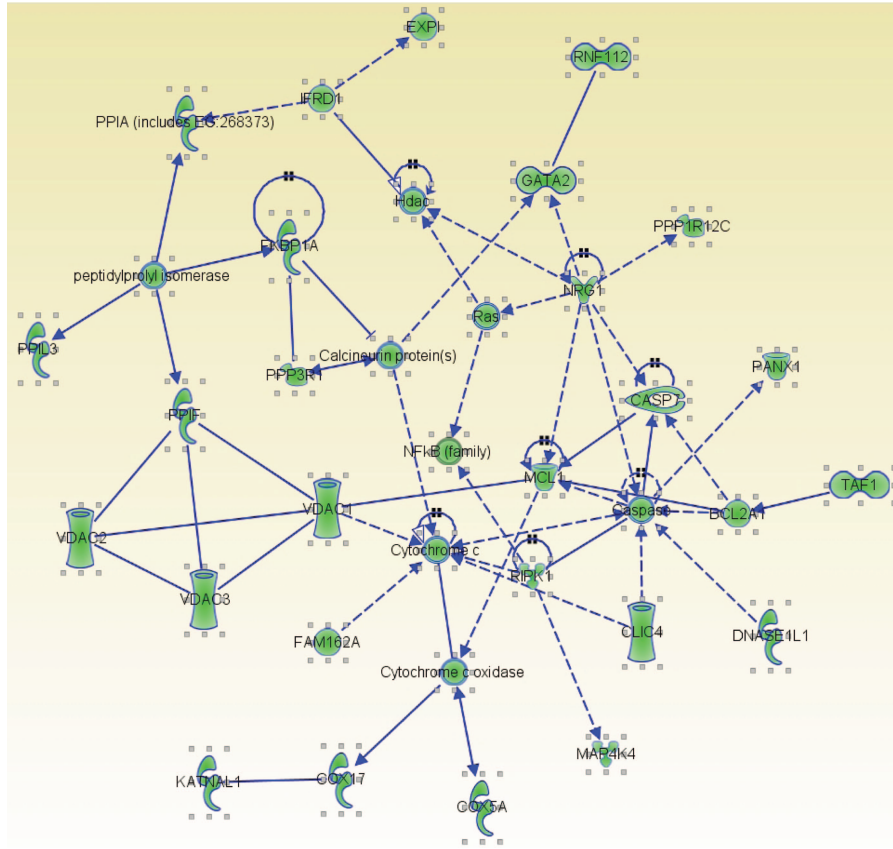

Figure 12. Cellular movement network downregulated in injured animals.

GeneSpring 10.1 was used to functionally classify the genes associated with pathophysiology in various systems in treated animals. Ingenuity Pathway Analysis and GeneCite were also used to carry out detailed pathway analysis using the BioCarta pathways.[11] Through functional classification and pathway analysis of upregulated genes, it was revealed that genes involved in dermatological disease and connective tissue networks demonstrated upregulation in treated animals vs control animals (Figures 10 and 11). Conversely, functional classification and analysis of downregulated genes showed cellular movement networks and signaling and nervous system networks as being the top-ranked downregulated networks (Figures 12 and 13).

Ingenuity analysis of the genes upregulated in injured animals vs controls identified, as part of the enriched connective tissue-related network, genes coding for various calcium channels and glutathione transferase. A robust cohort of genes demonstrating upregulation that are part of the enriched connective tissue network were found, as well as the genes upregulated and involved in the enriched dermatological network.

Downregulated genes included in the downregulated cellular movement pathway included RNA polymerases. Those within the signaling and nervous system network included nuclear factor kappa-light-chain-enhancer of activated B cells (NFκB), members of the cyclooxygenase (COX) family, caspases, and both cytochrome C and cytochrome C oxidase.

DISCUSSION

A novel model has been developed for the study of contact electrical injury that allows for the measurement of perfusion metrics near injury sites and simultaneous measurement of systemic molecular markers of injury. Other studies have focused on elucidating the cellular mechanism for tissue destruction including Joule heating, cellular membrane destruction, and other biophysical perturbations.[12–17] Forward looking infrared images were obtained in this model. Work is ongoing in attempts to align these images with perfusion maps to capture information about heat trajectories and the correlation between surface heating and tissue damage.

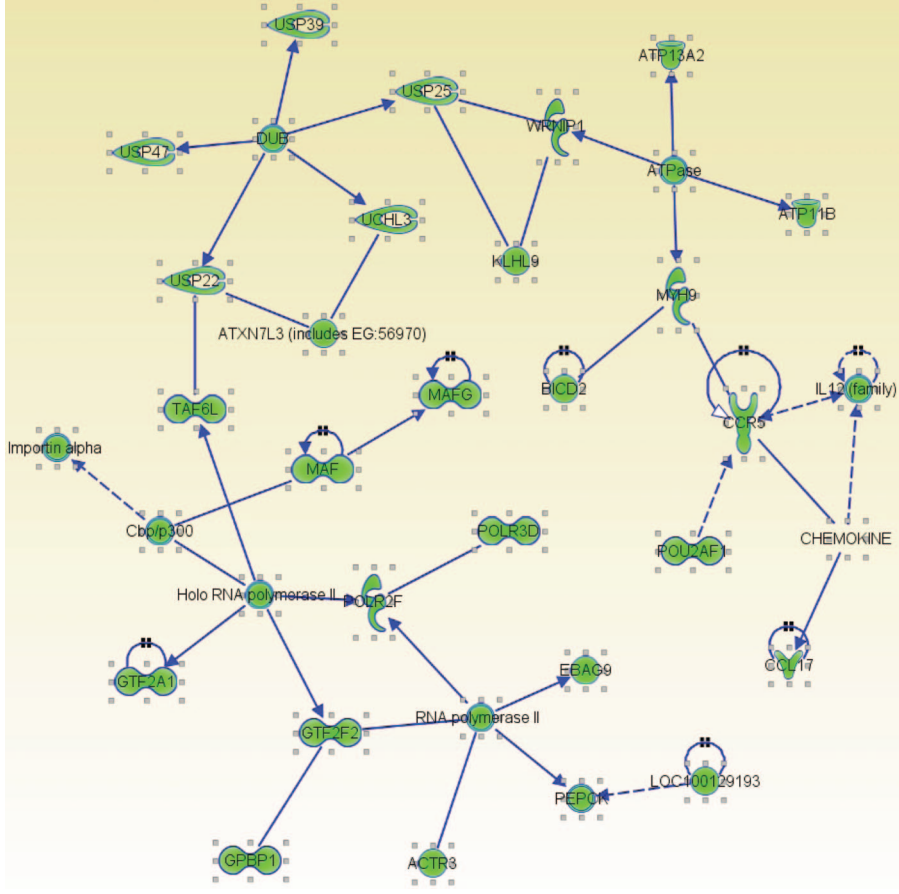

Figure 13. Nervous system signaling downregulated network in injured animals.

A dose-dependent increase was observed in injury severity and none of the tested conditions resulted in animal death. Cardiac dysfunction at the time of injury was not assessed by electrocardiography. However, it is unlikely that the animals experienced prolonged arrhythmia as gross assessments of global perfusion did not change after injury and animals did not require cardiovascular support.

In less severe wounds (upper extremity), perfusion indices in the tissues adjacent to wounds showed a biphasic response. Near the cathode injury sites, there was a reduction in this response for the shorter exposure groups and hyperperfusion was induced for all others. Taken together, these perfusion data show promise for applications in determining the severity of injury to underlying tissue proximal to contact wounds. Future work will be focused to follow these areas over a longer time course and to compare these data to that of histologic examination as well as other noninvasive imaging modalities such as spectral imaging, in vivo confocal microscopy, and optical coherence tomography.

Protein evaluation showed variable results, likely because specimens were recovered too proximal to injury to allow for most protein pathways to yield differential concentrations. It is likely difficult to capture systemic response at the protein level within 3 hours of injury, and future work is aimed at augmenting the current model to allow for a survival model that will allow for assessment at hours 12, 24, and 48 postinjury. Two proteins did show significant changes when values from control and injured animals were compared. IL-10 is an important cytokoine involved in the anti-inflammatory response to injury.[18] It is produced and released by monocytes, macrophages, and T-lymphocytes. In electrically injured animals, the levels of IL-10 were as high as threefold that of control animals and were most elevated immediately after injury. In patients with large thermal injury, excess levels of IL-10 have been associated with increased mortality.[19] VEGF levels were blunted in injured animals while control animals had increasing concentrations over time. In control animals, this is likely the result of the ischemia to the noninjured limb (from arterial and venous catheter insertion). Potentially, VEGF levels continue to be elevated in these animals as tributaries and alternative pathways for blood flow are used. It is hypothesized that this response was inhibited in animals that sustained injury. A longer time course and modification of central vascular access will help elucidate this further.

Pathway analysis from data obtained through examination of differential mRNA levels provided interesting information. Connective tissue, neurological, and dermatological networks were all found to be differentially involved. The investigation into the cross-talk between these genes will provide a springboard for future investigation. Targeted analysis using RT-PCR will be directed at key regulators in the aforementioned pathways.

ACKNOWLEDGMENTS

We thank Dr. Mete for her expert statistical consultation. Funding for this work was generously provided by PEPCO Holdings, Inc. and the D.C. Firefighters Burn Foundation.

REFERENCES

1. Blackwell N, Hayllar J. A three year prospective audit of 212 presentations to the emergency department after electrical injury with a management protocol. Postgrad Med J 2002;78:283–5.
2. Lucas J. Electrical fatalities in Northern Ireland. Ulster Med J 2009;78:37–42.
3. Maghsoudi H, Adyani Y, Ahmadian N. Electrical and lightning injuries. J Burn Care Res 2007;28:255–61.
4. Koumbourlis AC. Electrical injuries. Crit Care Med 2002;30: S424–30.
5. Ackerman LL, Ryken TC, Kealey GP, Traynelis VC. Onset of symptomatic hydrocephalus requiring emergency cerebrospinal fluid diversion following high-voltage electrical burn injury. J Neurosurg 2010;112:394–8.
6. Block TA, Aarsvold JN, Matthews KL II, et al. The 1995 Lindberg Award. Nonthermally mediated muscle injury and necrosis in electrical trauma. J Burn Care Rehabil 1995;16:581–8.
7. Fan KW, Zhu ZX, Den ZY. An experimental model of an electrical injury to the peripheral nerve. Burns 2005;31: 731–6.
8. Kalkan T, Demir M, Ahmed AS, et al. A dynamic study of the thermal components in electrical injury mechanism for better understanding and management of electric trauma: an animal model. Burns 2004;30:334–40.
9. Cela CJ, Lee RC, Lazzi G. Modeling cellular lysis in skeletal muscle due to electric shock. IEEE Trans Biomed Eng 2011; 58:1286–93.
10. Benjamini Y, Hochberg Y. Controlling the false discovery rate: a practical and powerful approach to multiple tests. J R Stat Soc Series B Stat Methodol 1995;57:289–300.
11. Hammamieh R, Chakraborty N, Wang Y, et al. GeneCite: a stand-alone open source tool for high-throughput literature and pathway mining. OMICS 2007;11:143–51.
12. Lee RC, Astumian RD. The physicochemical basis for thermal and non-thermal 'burn' injuries. Burns 1996;22:509–19.
13. Lee RC, Canaday DJ, Doong H. A review of the biophysical basis for the clinical application of electric fields in soft-tissue repair. J Burn Care Rehabil 1993;14:319–35.
14. Lee RC, Gaylor DC, Bhatt D, Israel DA. Role of cell membrane rupture in the pathogenesis of electrical trauma. J Surg Res 1988;44:709–19.
15. Lee RC, Kolodney MS. Electrical injury mechanisms: electrical breakdown of cell membranes. Plast Reconstr Surg 1987; 80:672–9.
16. Lee RC, Kolodney MS. Electrical injury mechanisms: dynamics of the thermal response. Plast Reconstr Surg 1987;80: 663–71.
17. Lee RC, Zhang D, Hannig J. Biophysical injury mechanisms in electrical shock trauma. Annu Rev Biomed Eng 2000;2: 477–509.
18. Sabat R, Grutz G, Warszawska K, et al. Biology of interleukin-10. Cytokine Growth Factor Rev 2010;21:331–44.
19. Csontos C, Foldi V, Palinkas L, et al. Time course of pro- and anti-inflammatory cytokine levels in patients with burns—prognostic value of interleukin-10. Burns 2010;36:483–94.